Coding Efficiency for Different Switched-Mode RF Transmitter Architectures

Thomas Blocher
Christian Doppler Laboratory for Nonlinear Signal Processing
Graz University of Technology, Austria
Email: thomas.blocher@tugraz.at

Peter Singerl
Infineon Technologies Austria AG
Email: peter.singerl@infineon.com

***Abstract*— Conventional RF transmitters with power amplifiers in e.g. Class-AB operation provide only moderate electrical efficiencies for complex modulated signals. To increase the overall efficiency considerably, we can employ switched-mode power amplifiers (SMPA) with an appropriate baseband signal processing. Such efficient SMPAs generate a lot of spectral out-of-band components, which has to be attenuated by a bandpass filter before the signal is fed to the transmit antenna. Unfortunately, this impacts the electrical efficiency because these unwanted signal components are usually dissipated within the transmitter. A measure for the electrical efficiency degradation for complex modulated signals in a switched-mode operation is the coding efficiency. In this paper we develop different switched-mode transmitter architectures based on baseband PWM coding and analyze the coding efficiencies for different signal statistics.**

I. Introduction

Modern wireless communication systems are usually designed for high spectral efficiency. This leads to modulation formats with highly fluctuating signal envelopes with large peak-to-average power ratios (PAP). In order to comply with the spectral masks and the linearity requirements imposed by regulatory bodies, the RF power amplifier (PA) is usually backed off from the 1dB compression point. This PA operation generally results in a poor electrical efficiency [1], [2]. One common method to increase the efficiency is to linearize the nonlinear behavior of the RF PA with e.g. digital predistortion or feed-forward concepts, which allows the use of a larger range of the input-output power characteristics of the PA [2], [3]. Unfortunately the efficiency of such a linearized PA is still limited, and especially for high frequency applications far away from the theoretical limit of an ideal Class-B PA.
Switched-mode power amplifiers (SMPA) like Class-F, Class-D or Class-J [4], [1] give us the potential to increase the efficiency considerably because the active devices are operated as switches instead of current sources as in conventional quasi-linear amplifiers. To drive these amplifiers in an efficient way we need special modulators which encode the amplitude varying signals into pulses (e.g, varying duty-cycles or varying pulse densities) with constant amplitude to provide in each of the operating points (switch on or off) the maximum efficiency [5]. One of the major drawbacks of this coding scheme is the generation of unwanted out-of-band power which is converted into heat by the isolator which is located between the SMPA and the bandpass filter to maintain linearity as shown in Fig. 1.

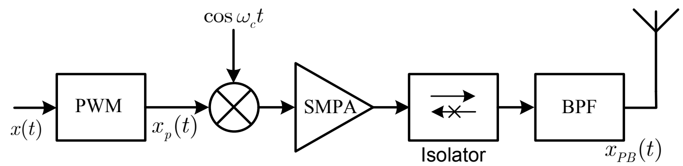

Fig. 1. Block diagram of a simple switched-mode transmitter (for real signals) with a baseband pulse-width modulator (PWM)

The dissipated power in the isolator reduces the electrical efficiency of the PA for non-constant envelope signals by the coding efficiency of the modulator.

II. Electrical Efficiency and Coding Efficency

Fig. 1 shows a simple block diagram of a switched-mode transmitter including a baseband pulse-width modulator. The real baseband signal $x(t)$ is encoded into 3-level pulses with variable length DT_p, where T_p is the fixed time period determined by a reference signal inside the PWM block. The encoded real baseband signal is composed in the ideal case of the original baseband input signal $x(t)$ and some distortion $d(t)$ whose frequency components are outside the band of interest [6]. To drive the SMPA in Fig. 1 we have to multiply the PWM output signal $x_p(t) = x(t) + d(t)$ with the desired carrier to obtain the RF bursts as shown in Fig. 2. The carrier inside the RF bursts switches the transistors of the SMPA on and off in a highly efficient way. During the off-time of the baseband pulses $x_p(t)$ the SMPA provides also high efficiency because the SMPA is completely switched off. After efficient power amplification of the RF bursts in the SMPA we have to recover the wanted passband signal with varying envelope $x_{PB}(t) = x(t)\cos(\omega_c t)$ before we feed the signal to the antenna. This is accomplished by a narrowband bandpass filter (BPF) centered around the carrier frequency, which reflects the unwanted out-of-band power back to the isolator, where it is dissipated. The dissipated power in the isolator reduces the electrical efficiency which is defined by the ratio of the filtered RF power (after the BPF) to the power drawn from the DC supply by

$$\eta_{el} = \eta_c \eta_{max}, \tag{1}$$

where the coding efficiency $\eta_c = P_{in}/P_{tot}$ is defined as the ratio of the wanted RF inband power (after the BPF)

978-1-4244-4480-9/09/$25.00

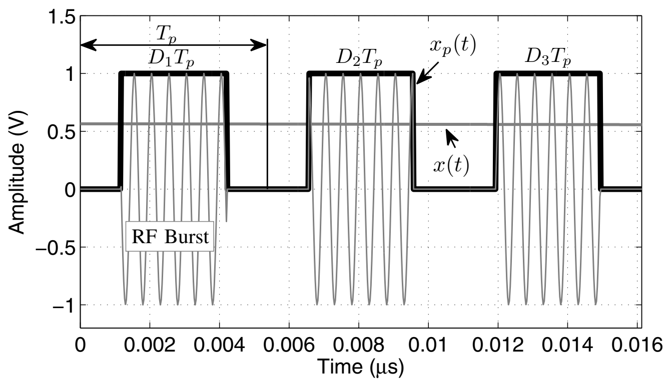

Fig. 2. Time-domain signals for the switched-mode transmitter in Fig. 1

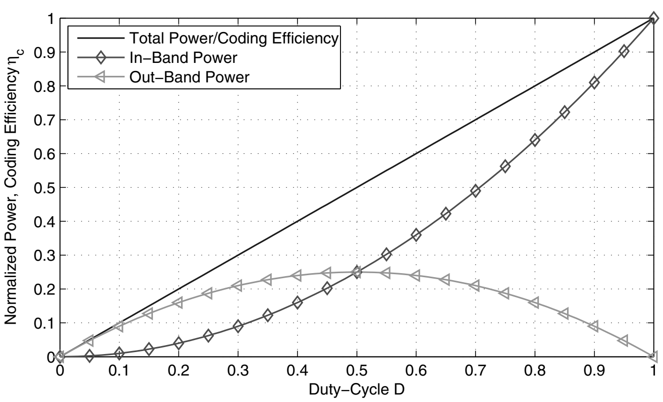

Fig. 3. The curves shows the normalized RF inband power P_{in} (diamond), the normalized RF outband power $P_{tot} - P_{in}$ (triangle), the normalized total RF power (solid) and the coding efficiency η_c (solid).

to the total power of the RF bursts (before the BPF). The electrical efficiency η_{max} describes the maximum efficiency of the SMPA for constant envelope operation which is usually in the range of 70%-80% [7], [8].

The total power of the RF bursts in Fig. 2 is calculated by $P_{tot} = 1/2D$ where D is the duty-cycle for the constant input signal $x = D, x \in [0, 1]$. This is practically true if the carrier frequency is much higher than the PWM frequency. The inband power of the RF bursts can be calculated from the mean value of PWM baseband signal by $P_{in} = 1/2D^2$ which gives the coding efficiency [9], [10], [5] by

$$\eta_c = \frac{P_{in}}{P_{tot}} = D. \tag{2}$$

Fig. 3 shows the normalized inband power P_{in}, the normalized total power P_{tot}, the normalized outband power $P_{tot} - P_{in}$ and the linear coding efficiency from (2) for varying constant input signals (duty-cycle).

For random input signals, the duty-cycles D_k of the PWM output signal $x_p(t)$ are changing from period to period in a random way according to the magnitude of the input signal $|x(t)|$. Therefore the total power of the RF bursts can be calculated by averaging the duty-cycles D_k which results in

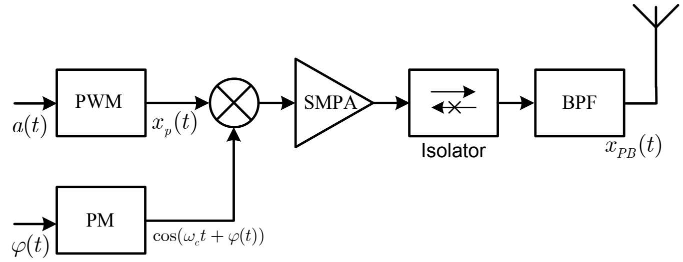

Fig. 4. Block diagram of a switched-mode polar transmitter with baseband PWM

$P_{tot} = 1/2\, E\{D_k\}$, where $E\{\cdot\}$ denotes the statistical expectation operator. If the random input signal $x(t)$ is sufficiently long, then the probability distribution function of the duty-cycles is equal to the probability distribution function of $|x(t)|$. Therefore the total power can be calculated by

$$P_{tot} = \frac{1}{2} E\{|x(t)|\}. \tag{3}$$

If we feed the RF bursts to the bandpass filter in Fig. 1, we obtain the wanted amplitude modulated signal $x_{PB}(t) = x(t)\cos\omega_c t$, whose power is calculated by

$$P_{in} = \frac{1}{2} E\{x^2(t)\}. \tag{4}$$

The coding efficiency for random input signal is now calculated with (3) and (4) by

$$\eta_c = \frac{E\{x^2(t)\}}{E\{|x(t)|\}}. \tag{5}$$

III. Switched-mode Transmitter with Baseband PWM Coding

Most of today's wireless communication standards are based on higher order complex modulation schemes with time varying magnitude information $a(t)$ and phase information $\phi(t)$ respectively. Fig. 4 depicts a polar switched-mode transmitter, where the magnitude information $a(t) = \sqrt{x_r^2(t) + x_i^2(t)}$ is encoded into a binary pulse-width modulated signal $x_p(t) = a(t) + d(t)$ as shown in Fig. 2 (time-domain) and Fig. 5 (frequency-domain) respectively. To drive the SMPA in Fig. 4 in an efficient way, the output signal of the PWM block $x_p(t)$ is multiplied with the phase modulated carrier $\cos(\omega_c t + \phi(t))$. The RF carrier is generated with the phase signal $\phi(t) = \arctan(x_i(t)/x_r(t))$ within the phase modulator (PM). During the on-time of $x_p(t)$ the phase modulated carrier is efficiently amplified in the SMPA and during the off-time of $x_p(t)$ the SMPA is switched off. The broadband spectrum of the RF bursts is depicted in Fig. 6. The desired modulated signal $a(t)\cos(\omega_c t + \phi(t))$ can be recovered with high SNR by a bandpass filter centered around the carrier frequency, if the PWM frequency is sufficiently high. Typically, the PWM frequency is 10-100 times the baseband bandwidth of the input signal.

To calculate the coding efficiency we have to determine the probability density function for the magnitude $a(t)$. If we assume that the real and imaginary component functions $x_r(t)$

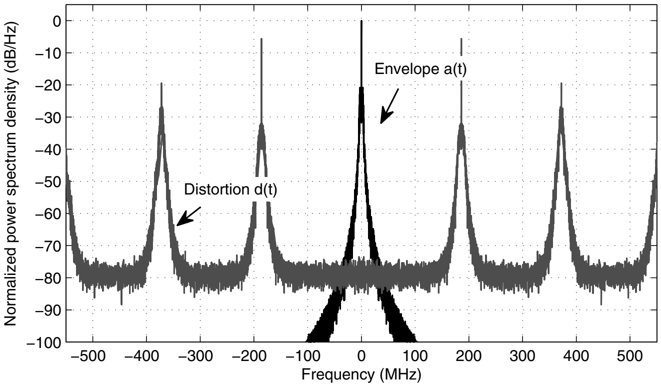

Fig. 5. Baseband spectrum of the PWM output signal $x_p(t) = a(t) + d(t)$ for the switched-mode polar transmitter in Fig. 4

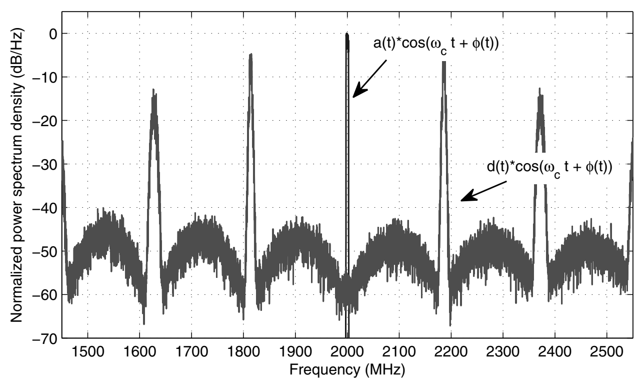

Fig. 6. Spectrum of the RF bursts $x_p(t)\cos(\omega_c(t) + \phi(t))$ for the switched-mode polar transmitter in Fig. 4

and $x_i(t)$ are Gaussian than the magnitude become Rayleigh distributed [11] as $f_r(a) = a/\sigma^2 \exp\left(\frac{-a^2}{2\sigma^2}\right)$. Therefore the coding efficiency for a clipped magnitude (to one) is given with (5) by

$$\begin{aligned}\eta_{c\ \text{Rayleigh}} &= \frac{E\left\{a^2\right\}}{E\left\{a\right\}} = \frac{\int_0^1 a^2 f_r(a)\,da + \int_1^\infty f_r(a)\,da}{\int_0^1 a f_r(a)\,da + \int_1^\infty f_r(a)\,da} \\ &= \frac{2\sigma^2 - 2\sigma^2 \exp\left(\frac{-1}{2\sigma^2}\right)}{\sqrt{\frac{\sigma^2\pi}{2}}\operatorname{erf}\left(\frac{1}{\sqrt{2\sigma^2}}\right)}. \qquad (6)\end{aligned}$$

The peak-to-average power ratio defined by PAP $= 10\log\left(\frac{\max\{a^2\}}{E\{a^2\}}\right)$ is calculated for the clipped Rayleigh magnitude distribution with $\max\{a^2\} = 1$ by

$$\begin{aligned}\text{PAP}_{\text{Rayleigh}} &= 10\log\left(\frac{1}{\int_0^1 a^2 f_r(a)\,da + \int_1^\infty f_r(a)\,da}\right) \\ &= 10\log\left(\frac{1}{2\sigma^2 - 2\sigma^2\exp\left(\frac{-1}{2\sigma^2}\right)}\right). \qquad (7)\end{aligned}$$

If the parameter $\sigma^2 << 1$, the coding efficiency in (6) and the

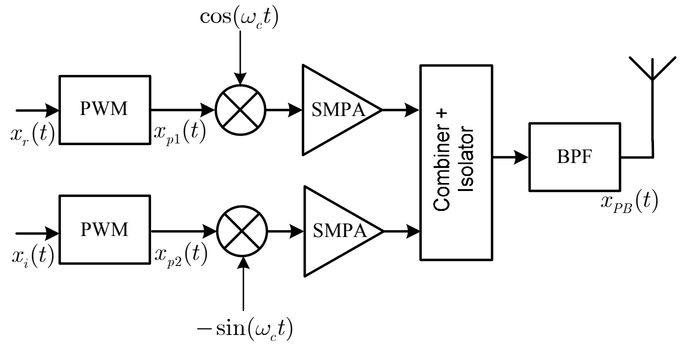

Fig. 7. Block diagram of a switched-mode IQ-transmitter with baseband PWM

PAP in (7) can be simplified by

$$\eta_{c\ \text{Rayleigh}} \approx \frac{\int_0^\infty x^2 f_r(x)\,dx}{\int_0^\infty x f_r(x)\,dx} = \frac{2\sigma^2}{\sqrt{\frac{\sigma^2\pi}{2}}} = \sqrt{\frac{\sigma^2 8}{\pi}} \qquad (8)$$

and

$$\text{PAP}_{\text{Rayleigh}} \approx 10\log\left(\frac{1}{2\sigma^2}\right). \qquad (9)$$

Now the coding efficiency in (8) can be calculated with (9) by

$$\eta_{c\ \text{Rayleigh}} \approx \sqrt{\frac{4}{\pi 10^{\text{PAP}_{\text{Rayleigh}}/10}}}. \qquad (10)$$

In Fig. 7 an alternative switched-mode transmitter based on an IQ-architecture is depicted. In contrast to the switched-mode polar transmitter in Fig. 4 the I- and Q-component signals $x_r(t)$ and $x_i(t)$ are separately encoded into PWM modulated signals as shown in Fig. 2. Because the I- and Q-signals are strictly band-limited, the PWM rate can be kept lower compared to the polar transmitter where the ideal non band-limited magnitude $a(t)$ (see Fig. 5) is encoded to the PWM signal $x_p(t)$. This results in less switching losses within the SMPA and therefore in a higher electrical efficiency. One of the drawbacks with this switched-mode transmitter architecture is the increased hardware demand compared to the polar transmitter shown in Fig. 4 because in general two SMPAs and an additional power combiner are needed. The signal combination cannot be accomplished before the SMPA in general (only one SMPA is needed), because the independent RF bursts from the I- and Q-path would interfere to a multi-level SMPA driving signal.

If we assume that the I- and Q-signals in Fig. 7 are independent and Gaussian distributed with $f_g(x) = \frac{1}{\sqrt{2\pi\sigma^2}}\exp\left(\frac{-x^2}{2\sigma^2}\right)$, the coding efficiency is given by

$$\begin{aligned}\eta_{c\ \text{Gauss}} &= \frac{E\left\{x^2\right\}}{E\left\{|x|\right\}} = \frac{\int_0^1 x^2 f_g(x)\,dx + \int_1^\infty f_g(x)\,dx}{\int_0^1 x f_g(x)\,dx + \int_1^\infty f_g(x)\,dx} \\ &= \frac{1 + \operatorname{erf}\left(\frac{1}{\sqrt{2\sigma^2}}\right)\left(\sigma^2 - 1\right) - \sqrt{\frac{2\sigma^2}{\pi}}\exp\left(\frac{-1}{2\sigma^2}\right)}{\sqrt{\frac{2\sigma^2}{\pi}}\left(1 - \exp\left(\frac{-1}{2\sigma^2}\right)\right) + 1 - \operatorname{erf}\left(\frac{1}{\sqrt{2\sigma^2}}\right)}. \qquad (11)\end{aligned}$$

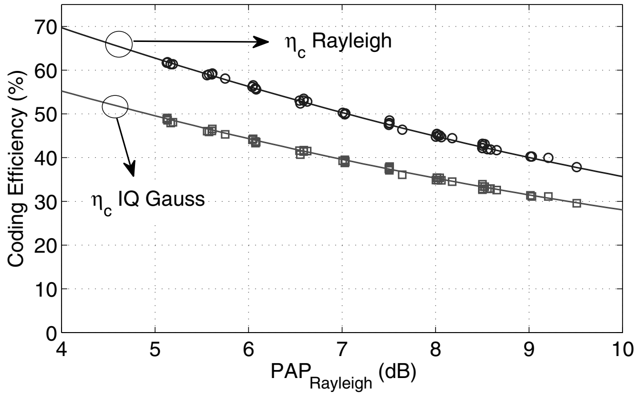

Fig. 8. Coding efficiencies for the switched-mode polar transmitter (Rayleigh distribution) and switched-mode IQ-transmitter (Gaussian distribution). The solid lines show the calculated efficiencies, the markers show the simulation results

The PAP for the Gaussian distributed signal is computed by

$$\begin{aligned}\text{PAP}_{\text{Gauss}} &= 10\log\left(\frac{1}{2\int_0^1 x^2 f_g(x)\,dx + 2\int_1^\infty f_g(x)\,dx}\right)\\ &= 10\log\left(\frac{1}{1+\text{erf}\left(\frac{1}{\sqrt{2\sigma^2}}\right)(\sigma^2-1) - \sqrt{\frac{2\sigma^2}{\pi}}\exp\left(\frac{-1}{2\sigma^2}\right)}\right).\end{aligned} \tag{12}$$

If the parameter $\sigma^2 << 1$, the coding efficiency in (11) and the PAP in (12) can be approximated by

$$\eta_{c\ \text{Gauss}} \approx \frac{\int_0^\infty x^2 f_g(x)\,dx}{\int_0^\infty x f_g(x)\,dx} = \sqrt{\frac{\sigma^2\pi}{2}} \tag{13}$$

and

$$\text{PAP}_{\text{Gauss}} \approx 10\log\left(\frac{1}{\sigma^2}\right) = \text{PAP}_{\text{Rayleigh}} + 3. \tag{14}$$

Now the coding efficiency in (13) can be calculated with (14) and (9) by

$$\eta_{c\ \text{Gauss}} \approx \sqrt{\frac{\pi}{2\cdot 10^{(\text{PAP}_{\text{Rayleigh}}+3)/10}}}. \tag{15}$$

Fig. 8 shows the calculated coding efficiencies $\eta_{c\ \text{Rayleigh}}$ and $\eta_{c\ \text{Gauss}}$ for the switched-mode polar transmitter in Fig. 4 and the switched-mode IQ-transmitter in Fig. 7 as well. The solid lines depict the theoretical coding efficiencies and the markers show the corresponding simulation results. It is important to note that the coding efficiency and therefore also the electrical efficiency for the switched-mode polar transmitter is always better than the corresponding efficiencies for the switched-mode IQ-transmitter. The price paid for the higher coding efficiency is the higher PWM rate, which is needed to encode the magnitude $a(t)$ into a corresponding pulse sequence $x_p(t)$ which is suitable to drive the SMPA.

IV. Conclusion

Switched-mode power amplifiers have the potential to increase the electrical efficiency considerably. Because these amplifiers are operated as switches instead of controlled current sources, the magnitude information of the modulated signal must be encoded into pulses to be able to drive the SMPA in an efficient way. The encoding of the amplitude information generates spectral out-of-band components which are normally dissipated within the transmitter (SMPA, Isolator,...). The coding efficiency which is defined as the ratio of the desired inband power to the total power generated by the SMPA, is a measure for the electrical efficiency in a back-off operation. We have investigated different switched-mode transmitter architectures including the required baseband processing. We have analyzed the coding and the electrical efficiencies for these architectures respectively. Furthermore we have shown that a switched-mode polar transmitter is superior compared to alternative transmitter architectures in terms of efficiencies and the lower demand on analog RF components.

References

[1] S. C. Cripps, *RF Power Amplifiers for Wireless Communications, Second Edition*. Norwood, MA, USA: Artech House, Inc., 2006.

[2] F. Raab, P. Asbeck, S. Cripps, P. Kenington, Z. Popovic, N. Pothecary, J. Sevic, and N. Sokal, "Power amplifiers and transmitters for RF and microwave," *Microwave Theory and Techniques, IEEE Transactions on*, vol. 50, no. 3, pp. 814–826, Mar 2002.

[3] A. Katz, "Linearization: reducing distortion in power amplifiers," *Microwave Magazine, IEEE*, vol. 2, no. 4, pp. 37–49, Dec 2001.

[4] F. H. Raab, P. Asbeck, S. Cripps, P. B. Kenington, Z. B. Popovic, N. Pothecary, J. F. Sevic, and N. O. Sokal, "RF and microwave power amplifier and transmitter technologies part 2," *High Frequency Electronics*, vol. 2, no. 4, pp. 22–36, May 2003.

[5] Y.-S. Jeon, H.-S. Yang, and S. Nam, "A novel high-efficiency linear transmitter using injection-locked pulsed oscillator," *Microwave and Wireless Components Letters, IEEE*, vol. 15, no. 4, pp. 214–216, April 2005.

[6] Z. Song and D. V. Sarwate, "The frequency spectrum of pulse width modulated signals," *Signal Process.*, vol. 83, no. 10, pp. 2227–2258, 2003.

[7] F. Lepine, A. Adahl, and H. Zirath, "L-band LDMOS power amplifiers based on an inverse class-F architecture," *Microwave Theory and Techniques, IEEE Transactions on*, vol. 53, no. 6, pp. 2007–2012, June 2005.

[8] H. Nemati, C. Fager, and H. Zirath, "High efficiency LDMOS current mode class-D power amplifier at 1 GHz," *Microwave Conference, 2006. 36th European*, pp. 176–179, Sept. 2006.

[9] T. Johnson and S. Stapleton, "Available load power in a RF class D amplifier with a sigma-delta modulator driver," *Radio and Wireless Conference, 2004 IEEE*, pp. 439–442, Sept. 2004.

[10] T. Johnson and S. P. Stapleton, "RF class-D amplification with bandpass sigmadelta modulator drive signals," *Circuits and Systems I: Regular Papers, IEEE Transactions on*, vol. 53, no. 12, pp. 2507–2520, Dec. 2006.

[11] A. Papoulis and S. U. Pillai, *Probability, Random Variables and Stochastic Processes*, fourth edition ed. Boston, Burr Ridge, IL, Dubuque, IA: McGraw-Hill, 2002.